HHS Public Access

Author manuscript

J Neurochem. Author manuscript; available in PMC 2018 April 11.

Published in final edited form as:

J Neurochem. 2016 November ; 139(3): 396–407. doi:10.1111/jnc.13767.

Cannabinoid receptor interacting protein suppress agonist–driven CB_1 receptor internalization and regulates receptor replenishment in an agonist–biased manner

Lawrence C. Blume[*], **Sandra Leone-Kabler**[*], **Deborah J. Luessen**[*], **Glen S. Marrs**[†,‡], **Erica Lyons**[*], **Caroline E. Bass**[*,1], **Rong Chen**[*,§], **Dana E. Selley**[§], and **Allyn C. Howlett**[*,‡]

[*]Department of Physiology and Pharmacology, Wake Forest University Health Sciences, Winston-Salem, North Carolina, USA

[†]Department of Biology, Wake Forest University, Winston-Salem, North Carolina, USA

[‡]Center for Molecular Signaling, Wake Forest University, Winston-Salem, North Carolina, USA

[§]Department of Pharmacology and Toxicology, Virginia Commonwealth University, Richmond, Virginia, USA

Abstract

Cannabinoid receptor interacting protein 1a (CRIP1a) is a CB_1 receptor (CB_1R) distal C-terminus-associated protein that modulates CB_1R signaling via G proteins, and CB_1R down-regulation but not desensitization (Blume *et al*. [2015] *Cell Signal*., 27, 716–726; Smith *et al*. [2015] *Mol. Pharmacol*., 87, 747–765). In this study, we determined the involvement of CRIP1a in CB_1R plasma membrane trafficking. To follow the effects of agonists and antagonists on cell surface CB_1Rs, we utilized the genetically homogeneous cloned neuronal cell line N18TG2, which endogenously expresses both CB_1R and CRIP1a, and exhibits a well-characterized endocannabinoid signaling system. We developed stable CRIP1a-over-expressing and CRIP1a-siRNA-silenced knockdown clones to investigate gene dose effects of CRIP1a on CB_1R plasma membrane expression. Results indicate that CP55940 or WIN55212-2 (10 nM, 5 min) reduced cell surface CB_1R by a dynamin- and clathrin-dependent process, and this was attenuated by CRIP1a over-expression. CP55940-mediated cell surface CB_1R loss was followed by a cycloheximide-sensitive recovery of surface receptors (30–120 min), suggesting the requirement for new protein synthesis. In contrast, WIN55212-2-mediated cell surface CB_1Rs recovered only in CRIP1a knockdown cells. Changes in CRIP1a expression levels did not affect a transient rimonabant (10 nM)-mediated increase in cell surface CB_1Rs, which is postulated to be as a result of rimonabant effects on ‘non-agonist-driven’ internalization. These studies demonstrate a novel role for CRIP1a in agonist-driven CB_1R cell surface regulation postulated to occur by two mechanisms: 1) attenuating internalization that is agonist-mediated, but not that in the absence of exogenous

Address correspondence and reprint requests to Allyn C. Howlett, PhD, Department of Physiology and Pharmacology, Wake Forest School of Medicine, Medical Center Blvd., Winston-Salem, NC 27157, USA. ahowlett@wakehealth.edu.

[1]Present address: Department of Pharmacology and Toxicology, School of Medicine and Biomedical Sciences, University at Buffalo, Buffalo, NY 14260, USA.

Conflict of interest disclosure

The authors declare that they have no conflicts of interest with the contents of this article.

agonists, and 2) biased agonist-dependent trafficking of de novo synthesized receptor to the cell surface.

Keywords

cannabinoid receptor interacting protein; CB_1 cannabinoid receptor; CP55940; receptor trafficking; rimonabant; WIN55212-2

The cannabinoid receptor interacting protein 1a (CRIP1a) is a CB_1 cannabinoid receptor (CB_1R)-associated protein, the function of which has remained elusive (Niehaus *et al.* 2007). Regulation by CRIP1a of cellular signaling has been indicated by recent studies. In the original identification of CRIP1a, it was shown that CB_1R-mediated tonic inhibition of N-type voltage-gated Ca^{2+} channels was inhibited by CRIP1a in superior cervical ganglion neurons (Niehaus *et al.* 2007). We showed that over-expression of CRIP1a in striatal cells reduced Extracellular Signal Regulated Kinase (ERK)1/2 phosphorylation (Blume *et al.* 2013). We also showed that CB_1 agonist-stimulated [^{35}S]GTPγS binding was attenuated by CRIP1a over-expression in HEK293 cells stably expressing CB_1R as well as in N18TG2 cells that endogenously express both CB_1R and CRIP1a, without affecting CB_1R expression levels in either cell line (Blume *et al.* 2015; Smith *et al.* 2015). These reductions in G-protein activation were associated with reductions in CB_1R signal transduction and downstream function in N18TG2 cells (Blume *et al.* 2015). Conversely, RNA interference-mediated knockdown of CRIP1a in N18TG2 cells generally produced opposite effects on CB_1R-mediated G-protein activation and signal transduction (Blume *et al.* 2015; Smith *et al.* 2015).

Although these studies suggest diverse roles for CRIP1a in CB_1R regulation, the underlying mechanisms involved in the modulation of CB_1R-mediated neuronal functions by CRIP1a are just beginning to be understood. Other associated proteins for CB_1R, such as G-protein-coupled receptor (GPCR) kinases, β-arrestins, adaptor protein 3 and GPCR-associated sorting protein 1 (GASP1), regulate CB_1R trafficking and localization (Howlett *et al.* 2010; Smith *et al.* 2010). In cell model systems, exogenously expressed CB_1R can undergo rapid (5 min) sequestration or internalization from the plasma membrane following agonist treatment (Hsieh *et al.* 1999; Coutts *et al.* 2001; Daigle *et al.* 2008). In this study, our primary focus was to determine the effects of CRIP1a on the regulation of CB_1R plasma membrane expression and trafficking during agonist and inverse agonist occupancy of the receptor.

To investigate the role of CRIP1a on CB_1R cell surface density, we employed both CRIP1a over-expression and RNA interference-induced CRIP1a knockdown in stably transfected clones of the N18TG2 neuronal cell line. We found that agonists promoted a rapid loss of cell surface CB_1R which was profoundly inhibited by the over-expression of CRIP1a. We also report an involvement of CRIP1a to suppress the re-establishment of cell surface CB_1R by *de novo* synthesis following prolonged agonist exposure, and that this effect was dependent on the agonist used. These studies are the first to identify a function for the CB_1R accessory protein CRIP1a in modulating changes in CB_1R cell surface localization in response to CB_1R activation.

Materials and methods

Materials

The National Institute of Drug Abuse drug supply program kindly provided CP55940 ((-)-*cis*-3R-[2-hydroxy-4-(1,1-dimethylheptyl) phenyl]-*trans*-4R-3(3-hydroxypropyl)-1R cyclohexanol and rimonabant (*N*-(piperidin-1yl)-5-(4-chlorophenyl)-1-(2,4-dichlorophenyl)-4-methyl-H-pyrazole-3-carboxamide). The sources for specialized compounds were WIN55212-2 ([2,3-dihydro-5-methyl-3-[(4-morpholinyl)methyl]pyrrolo[1,2,3-de]-1,4-benzoxazin-6-yl](1-naphthyl) methanone and tetrahydrolipstatin (THL, orlistat) from Cayman Chemical (Ann Arbor, MI, USA); dynasore (3-hydroxynaphthalene-2-carboxylic acid (3,4-dihydroxybenzylidene)hydrazide) from Tocris Biosciences (Minneapolis, MN, USA); chlorpromazine, cycloheximide and nystatin from Sigma-Aldrich (St. Louis, MO, USA).

Cell culture models

Culture conditions, mRNA and protein quantification of CB_1R and CRIP1a in N18TG2 neuronal wild-type (WT, untransfected) cells and stable clones selected for CRIP1a over-expression (XS 1 and XS 5) and siRNA-silencing knockdown (KD 2C and KD 2F) have been described previously (Blume *et al*. 2015; Smith *et al*. 2015). CRIP1a over-expressing N18TG2 clones have approximately a 2.3-to 2.5-fold increase in both CRIP1a protein expression and the CRIP1a : CB_1R expression ratio, in comparison to untransfected N18TG2 cells; however, in knockdown cells the molar ratio of CRIP1a:CB_1R could not be established due to low CRIP1a levels (Smith *et al*. 2015). Data are shown for an empty vector pcDNA3 clone (Control), as well as two different clones of each transgenic modification in order to reinforce that the effects observed were as a result of increasing or decreasing CRIP1a protein expression, rather than an aberration as a result of transfection and cloning processes.

Immunocytochemistry determination of cell surface CB_1R density

CB_1R cell surface density was quantified using a 96-well format 'On-cell-Western' immunocytochemistry assay, as reported previously (Miller 2004; Blume *et al*. 2015; Smith *et al*. 2015). Briefly, cells at 90% confluence were serum-starved (16 h), pretreated with 1 μM THL (2 h) to reduce 2-arachidonoylglycerol (2-AG) levels and indicated enzyme inhibitors were added 15 or 30 min prior to drug exposure. Cells were treated with vehicle, 10 nM CP55940, 10 nM WIN55212-2 or 10 nM rimonabant at 37°C for the indicated times. The reaction was terminated by placing plates on ice, washing with cold buffer and fixing with ice-cold 1.2% phosphate-buffered formalin (1.5 mM KH_2PO_4, 2.7 mM KCl, 8 mM Na_2HPO_4, 150 mM NaCl; 1.2% paraformaldehyde (v/v), pH 7.4) for 15 min at 4°C. Plates were washed three times for 5 min with phosphate-buffered saline (PBS) (1.5 mM KH_2PO_4, 2.7 mM KCl, 8 mM Na_2HPO_4, 150 mM NaCl, pH 7.4), blocked for 90 min in LI-COR blocking buffer and incubated with gentle rocking at 4°C for 18 h with goat anti-CB_1R (N15; Santa Cruz Biotechnology, Santa Cruz, CA, USA) targeting the amino terminus of CB_1R (1 : 800). Plates were then washed in PBS containing 0.1% Tween-20 and incubated simultaneously for 1 h with a secondary IR Dye 800CW donkey anti-goat (LI-COR Biosciences, Lincoln, NE, USA) (1 : 1500) and the nuclear stain DRAQ5 (1 : 5000) (Cell

Signaling Technology, Danvers, MA, USA) to normalize for well-to-well variations in cell density. Plates were washed four times with PBS Tween-20, and immunofluorescence was imaged using the LI-COR Odyssey (169 μm resolution, 5 sensitivity, 4.01235 mm offset, medium quality). Immunoreactive CB_1R fluorescence intensity was first normalized to DRAQ5 and then cell surface receptor values were quantified relative to WT at time 0 min (no agonist) expressed as 100%.

Imaging of endogenously expressed CB_1R

For imaging cell surface CB_1R (Fig. 2a), N18TG2 cells were plated on coverslips coated with 0.5 mg/mL poly-D-lysine (Sigma-Aldrich) inside wells of six-well plates. Cells that had been pretreated with THL in serum-free Dulbecco's modified Eagle's medium-Ham's F12 (2 h) were incubated with vehicle or CP55940 (10 nM) for 15 min at 37°C. To terminate the incubation, the medium was replaced with cold PBS, and coverslips were blocked with 4% normal donkey serum for 30 min on ice. Surface CB_1Rs were labeled at 4°C with goat anti-CB_1R antibody (N15; Santa Cruz Biotechnology), followed by incubation with secondary donkey anti-goat Alexa Fluor 633 (Invitrogen, Carlsbad, CA, USA). Coverslips were mounted with ProLong Gold Anti-fade reagent (Life Technologies, Grand Island, NY, USA) for imaging on a Zeiss LSM 710 laser scanning confocal microscope (639 oil immersion objective, 1.4 NA) and Zen Lite 2012™ software. All images shown were subjected to equal parameters in Adobe Photoshop for optimal presentation.

To quantitate internalization (Fig. 2b), cells were treated with vehicle or CP55940 (10 nM) for 5 min at 37°C, washed with cold PBS and blocked with 6% normal donkey serum. Surface CB_1Rs were labeled at 4°C with N15 goat anti-CB_1R N-terminal antibody followed by donkey anti-goat Alexa Fluor 633. To determine total CB_1Rs, cells were then fixed with 4% paraformaldehyde in PBS followed by permeabilization (0.1% Triton X-100 in PBS) for 10 min. Coverslips were quenched with 50 mM NH_4Cl in PBS for 20 min to minimize autofluorescence from paraformaldehyde. Subsequently, total CB_1Rs were labeled with a rabbit anti-CB_1R antibody targeting the C-terminus of the CB_1R (Pierce Biotechnology, Rockford, IL, USA), followed by goat anti-rabbit Alexa Fluor 405 (Invitrogen). To quantitate internalization shown on confocal images, surface CB_1R immunofluorescence emission intensity (excitation at 633 nm) was divided by total CB_1R immunofluorescence emission intensity (excitation at 405 nm) for each individual cell.

Statistical analyses

Statistical differences were tested using ANOVA with Bonferroni or Dunnett's *post hoc* tests. Comparisons between two groups were performed by Student's *t*-test (GraphPad Prism VI; GraphPad Software Inc., San Diego, CA, USA).

Results

CRIP1a influences CB_1R cell surface equilibrium and translocation

We previously observed that stable CRIP1a-over-expressing clones (XS 1 and XS 5) exhibited a cell surface CB_1R level that was 70–75% of WT (untransfected WT) N18TG2 neuroblastoma cells, a finding that might have accounted for the reduced CB_1R-mediated

cellular signaling (Blume *et al*. 2015; Smith *et al*. 2015). Based on these findings, we further developed stably expressing siRNA CRIP1a knockdown clones (KD 2C and KD 2F) in the N18TG2 cell line, and now use these model cell clones to test whether CRIP1a is involved in regulating agonist-driven translocation of cell surface CB_1R. As seen in Fig. 1a and b, CP55940 mediated a reduction in CB_1R surface density that reached equilibrium at 5 min in both WT (27 ± 3%) and empty vector control cells (28 ± 4%). Similarly, WIN55212-2 produced a robust loss of surface CB_1Rs in the first 5 min (35 ± 5%), and a reduced equilibrium in CB_1R membrane expression at 5–10 min (31 ± 5%) (Fig. 1c and d). CP55940-promoted loss of CB_1R surface expression in CRIP1a knockdown cells (KD 2C and KD 2F) (Fig. 1b) was not different from WT during the first 5 min (KD 2C: 35 ± 5%; KD 2F: 34 ± 5%), and remained constant for 30 min (KD 2C: 29 ± 6%; KD 2F: 26 ± 5%). CRIP1a KD cells behaved similarly to WT during WIN55212-2 treatment at 5 min (Fig. 1d) (KD 2C: 31 ± 5%; KD 2F: 27 ± 6%) or 15 min (KD 2C: 28 ± 4%; KD 2F: 25 ± 5%).

In contrast, in two individual clones that over-expressed CRIP1a, treatment with CP55940 resulted in a minimal loss in CB_1R cell surface levels at 5 min (Fig. 1a) (XS 1: 12 ± 4%; XS 5: 10 ± 5%), which remained constant for 45 min (time course extended, data not shown) (XS 1: 13 ± 4%; XS 5: 9 ± 5%). Over-expression of CRIP1a also reduced the extent of CB_1R cell surface loss evoked by WIN55212-2 at 5 min (XS 1: 14 ± 6%; XS 5: 13 ± 6%) (Fig. 1c), which remained constant at 30 min (time course extended, data not shown) (XS 1: 18 ± 5%; XS 5: 16 ± 6%). To corroborate the internalization dysfunction produced by CRIP1a over-expression using a complementary method, control and CRIP1a XS cells were visualized using confocal microscopy (Fig. 2a). CP55940 treatment of control cells for 15 min decreased CB_1Rs that were immunolabeled from the external surface, consistent with receptor relocation to a compartment having limited access to extracellular antibodies. In contrast, CRIP1a XS cells failed to exhibit a pronounced depletion of external surface CB_1R aggregates upon agonist stimulation. Quantification of extracellular CB_1Rs as a ratio of external surface to total CB_1R fluorescent intensity (Fig. 2b) indicated that CP55940 treatment resulted in only a 13% decrease in extracellular CB_1R level in CRIP1a XS compared with 31% in control cells.

Together, these studies indicate that cells over-expressing CRIP1a exhibit a lower steady-state cell surface level of CB_1Rs compared with WT cells. The converse is also true: cells that express less than endogenous CRIP1a levels exhibit a somewhat greater steady-state cell surface level of CB_1Rs compared with WT cells. Agonist-mediated reduction in cell surface CB_1R levels could indicate that agonists mediate a sequestration of CB_1Rs away from access to N-terminal targeting antibodies such as by internalization, which can occur at endogenously expressed CRIP1a levels (or lower). The finding that CRIP1a over-expression attenuated this process suggests that increasing the cellular levels of CRIP1a can exert a negative effect on a sequestration or internalization process.

CRIP1a affects agonist-mediated cell surface CB_1R depletion through dynamin and clathrin-dependent mechanisms

Internalization of surface receptors occurs mainly through two well-characterized structures, clathrin-coated invaginations and caveolae from lipid rafts (Drake *et al*. 2006). The GTPase

dynamin functions in both clathrin- and caveolae-mediated endocytosis (Gold *et al.* 1999; Mayor and Pagano 2007). To elucidate the internalization mechanism that CRIP1a over-expression suppresses, we blocked dynamin with the inhibitor dynasore and examined net cell surface CB_1Rs. Figure 3 shows that during dynamin blockade, there were no significant decreases in the cell surface levels of CB_1R after CP55940 (a–c)- or WIN55212-2 (d–f)-treatment over the 10 min time course versus time 0 (no agonist) for WT or control (a and d), CRIP1a XS (b and e) or CRIP1a KD (c and f) clones. After treatment with dynasore, the average reduction in cell surface CB_1R over the course of a 10-min treatment with CP55940 was only 8 ± 5% for WT cells and 7 ± 6% for control cells. These experiments indicate that the majority of CB_1Rs that were depleted from the plasma membrane in response to agonist treatment required dynamin. Dynasore treatment did not antagonize or augment the attenuation by CRIP1a of CP55940- or WIN55212-2-evoked loss of cell surface CB_1R over the 10 min time course, or beyond to 120 min (data not shown). The lack of additivity of CRIP1a over-expression with dynasore treatment implicates a dynamin-mediated CB_1R process being suppressed by both. Dynasore treatment did not affect the steady-state level of cell surface CB_1R in WT, control, CRIP1a XS or CRIP1a KD cells (a–f; 0 min, no agonist).

To ascertain which internalization or sequestration mechanism(s) play a role in the effects of CRIP1a over-expression on CP55940-promoted cell surface CB_1R depletion, we used chlorpromazine and nystatin to disrupt internalization mediated by clathrin and caveolae, respectively. In Fig. 4(a), pretreatment of WT and control cells with chlorpromazine, an effective inhibitor of clathrin-mediated internalization (Wang *et al.* 1993; Rejman *et al.* 2005), revealed that cell surface levels of CB_1R were only marginally reduced by CP55940 (WT, 5 min, 12 ± 4.2%) compared with untreated cells. Chlorpromazine also attenuated CP55940-mediated cell surface CB_1R loss in CRIP1a KD cells (Fig. 4c) (1–5 min, CRIP1a KD 2C, 14 ± 6.1%). Chlorpromazine neither antagonized nor augmented the attenuation of CP55940-mediated cell surface CB_1R depletion in CRIP1a XS cells (Fig. 4b: 1–5 min, CRIP1a XS 1, 11 ± 5.2%). The lack of additivity implicates a chlorpromazine-sensitive process and the mechanism affected by over-expression of CRIP1a as being contiguous or related processes.

Experiments have also demonstrated a role for lipid rafts in trafficking of anandamide-activated CB_1Rs to the lysosomal sorting pathway in human breast cancer MDA-MB-231 cells (Sarnataro *et al.* 2005) or in non-agonist-driven recycling of CB_1Rs in C6 glioma cells (Bari *et al.* 2005). We tested the role of CRIP1a in lipid raft sequestration and caveolar internalization. WT and control cells were preincubated with nystatin to sequester cholesterol and disrupt lipid rafts (Cuitino *et al.* 2005), and then treated with CP55940. These cells displayed a prominent loss in cell surface CB_1Rs (5 min, WT: 37 ± 5%; Control: 40 ± 6%), typical of that observed in the absence of nystatin (Fig. 4d). Similarly, pretreatment with nystatin did not alter the CP55940-mediated cell surface CB_1R depletion in CRIP1a KD cells (5 min, CRIP1a KD 2C: 40 ± 7%) (Fig. 4f). Nystatin treatment also failed to affect the attenuated CP55940-mediated CB_1R cell surface loss in CRIP1a over-expressing cells (Fig. 4e: 5 min, CRIP1a XS 1, 13 ± 4%). The failure of nystatin to alter the rate or extent of agonist-mediated cell surface changes in CB_1R does not support the involvement of a caveolar mechanism.

CRIP1a involvement in CB_1R cell surface translocation during prolonged ligand occupancy

After prolonged CP55940 exposure, a gradual and complete recovery of CB_1R surface expression occurred in WT cells (Fig. 5a and b). In WT or control cells, a return to pre-agonist steady-state levels (100%) was observed between 15 min and 120 min of CP55940 exposure. However, CRIP1a XS cells remained at 70% of WT levels during this prolonged CP55940 exposure. During the re-establishment of CB_1R cell surface density, CRIP1a KD cells showed a modest enhancement in CB_1R surface density relative to WT, returning to the same equilibrium levels above WT (120 min, WT: 96 ± 3%; KD 2C: 109 ± 4%; KD 2F: 116 ± 7%). These studies suggest that a recovery of CB_1R to the cell surface during prolonged CP55940 occupancy occurs by a mechanism that reaches the same CB_1R density as the pre-agonist levels. Furthermore, the steady-state CB_1R level achieved during recovery is related to the amount of CRIP1a expressed (i.e., higher than endogenous CRIP1a: lower CB_1R; lower than endogenous CRIP1a: higher CB_1R).

Unlike cells treated with CP55940, WT or control cells exposed to WIN55212-2 failed to re-establish pre-agonist surface levels of CB_1R during a 30-min to 120-min treatment period (Fig. 5c and d). After prolonged treatment with WIN55212-2, CB_1R surface expression remained at 25 ± 6% below the initial level in WT cells. In CRIP1a XS cells, CB_1R membrane expression remained significantly below the pre-WIN55212-2 WT densities (120 min, WT: 75 ± 5%; XS 1: 50 ± 6%; XS 5: 56 ± 5%). However, in CRIP1a KD cells, CB_1R cell surface density fully returned to pre-WIN55212-2 values (KD 2C: 109 ± 5%; KD 2F: 116 ± 5%) (Fig. 5d). Final steady-state CB_1R surface levels were significantly different between WT cells (120 min, WT: 78 ± 5%) and CRIP1a KD cells (120 min, KD 2C: 109 ± 6%; KD 2F: 112 ± 5%). These data suggest that there is an agonist-biased mechanism of establishing cell surface density of CB_1R, such that CRIP1a at endogenous levels or greater can suppress the level of cell surface receptors under the influence of WIN55212-2.

In order to characterize the mechanism(s) involved in re-establishing the cell surface density of CB_1R during prolonged agonist treatment, we examined whether new protein synthesis was required. The re-establishment of CB_1R surface density following prolonged CP55940 treatment (60–120 min) was significantly blocked in the presence of the protein synthesis inhibitor cycloheximide in WT and empty vector control cells (Fig. 6a) and CRIP1a KD (Fig. 6c). In CP55940-treated CRIP1a XS cells, a significant loss in CB_1R density at the cell surface was observed from 60 to 120 min treatment with cycloheximide (Fig. 6b). This demonstrates that *de novo* protein synthesis is required to maintain levels of CB_1R at the plasma membrane, independent of the degree of agonist-dependent CB_1R cell surface depletion.

In WIN55212-2-treated WT or control cells (Fig. 6d) or CRIP1a XS cells (Fig. 6e), cycloheximide reduced CB_1R surface density marginally (not significantly different from the absence of cycloheximide). However, cycloheximide abolished CB_1R cell surface re-population during 60 to 120 min WIN55212-2 exposure in CRIP1a KD cells (Fig. 6f), demonstrating that in the reduced CRIP1a environment, the recovery of cell surface CB_1R required new protein synthesis. In the described protocol, cycloheximide added 30 min prior to agonist challenge did not alter basal (pre-agonist) CB_1R cell surface levels in WT, control or the CRIP1a transgenic clones (Fig. 6a–f), or total CB_1R or CRIP1a protein expression

(data not shown). Of note, the presence of cycloheximide had no significant effect on the processes of agonist-mediated cell surface depletion (1–5 min) or the prolonged period of reduced steady-state levels (5–30 min) before recovery (Fig. 6a–f).

The CB_1 antagonist/inverse agonist rimonabant has been reported to promote and stabilize CB_1R cell surface expression postulated in those studies to be because of blocking non-agonist-driven 'constitutive' internalization of CB_1Rs (Rinaldi-Carmona *et al.* 1998; Leterrier *et al.* 2004; McDonald *et al.* 2007). In our studies, treatment of WT and control cells with rimonabant (10 nM) in the absence of agonists caused an increase in CB_1R surface expression over basal (5 min, WT: 114 ± 5%), which reached its peak at 15 min (133 ± 6%), before re-establishing the baseline levels at 60 min (106 ± 6%) (Fig. 7a and b). As shown in Fig. 7(a), an increase in CB_1R surface expression resulted following rimonabant treatment for CRIP1a XS (5 min, XS 1: 112 ± 5%; XS 5: 113 ± 6%), with maximal CB_1R surface expression occurring at 15 min (XS 1: 134 ± 5%; XS 5: 127 ± 8%). CRIP1a KD cells (Fig. 7b) also exhibited an observable increase at 5 min (KD 2C: 126 ± 4%; KD 2F: 128 ± 5%) and maximal surface expression at 15 min (KD 2C: 142 ± 5%; KD 2F: 141 ± 6%). For all cells that expressed CRIP1a at all levels, the CB_1R surface expression was re-established to steady-state WT levels after 120 min treatment with rimonabant. This means that the CRIP1a XS clones displayed an augmentation (~ 26%) in CB_1R surface expression after 120-min exposure to rimonabant compared with the initial levels in these clones (Fig. 7a), suggesting that the suppression of steady-state levels of CB_1R by CRIP1a over-expression can be relieved in the presence of rimonabant.

Discussion

Data presented here show that in the N18TG2 neuronal cell line, which endogenously expresses both CB_1R and CRIP1a at their native stoichiometry, agonist occupancy can reduce a pool of cell surface CB_1Rs within minutes. This pool is limited to only a fraction (30–40%) of surface CB_1Rs, and reaches a new equilibrium at the cell surface (from 5 min to 30 min) that remains below the pre-agonist cell surface levels until *de novo* synthesized receptors appear on the plasma membrane. Previous studies indicated that both CB_1R and CRIP1a appeared predominantly in Na/K-ATPase-containing membranes from the N18TG2 cells, with a smaller fraction of both proteins in an NP40-insoluble, caveolin 1-containing fraction (Blume *et al.* 2015). The data herein demonstrate that agonist-stimulated CB_1R cell surface depletion occurs via a dynamin-dependent process in a nystatin-resistant mechanism. The majority of cell surface loss occurred via a chlorpromazine-sensitive mechanism, consistent with the majority of agonist-dependent sequestration or internalization occurring from clathrin-coated pits. Our studies focused on the ability of the small associated protein CRIP1a to modulate these processes.

Our data support the premise that over-expression of CRIP1a can suppress the agonist-driven CB_1R sequestration or internalization processes. This finding can have relevant implications for cells that express CRIP1a, because in GPCRs that undergo internalization and trafficking to distinct intracellular compartments, deficits in GPCR internalization can affect signaling pathway selectivity (Drake *et al.* 2006; Hanyaloglu and von Zastrow 2008). In many cell types, GPCRs are directed into the recycling pathway for re-sensitization and

return to the plasma membrane, or to lysosomes for termination of receptor signaling via degradation (Drake *et al.* 2006; Hanyaloglu and von Zastrow 2008). Mechanisms responsible for agonist-dependent CB_1R internalization have been reported to involve a sequence of events including the activation of GPCR kinases, and the subsequent recruitment of β-arrestin2 (Hsieh *et al.* 1999; Daigle *et al.* 2008; Stadel *et al.* 2011; Nguyen *et al.* 2012). CB_1Rs have been shown to rapidly internalize following a short (5 min) exposure to a CB_1R agonist in AtT20 cells (Hsieh *et al.* 1999; Jin *et al.* 1999), HEK293 cells (Leterrier *et al.* 2004) and hippocampal neurons (Coutts *et al.* 2001; Leterrier *et al.* 2006). Elegant studies using live cell total internal reflection fluorescence microscopy have indicated that agonists can selectively retain CB_1R-β-arrestin complexes in clathrin-coated pits at the cell surface prior to internalization (Flores-Otero *et al.* 2014; Delgado-Peraza *et al.* 2016). CB_1R internalization requires dynamin as evidenced by the impairment of receptor endocytosis in cultured hippocampal neurons expressing dominant-negative dynamin isoforms (Leterrier *et al.* 2006). Hsieh *et al.* (1999) were the first to report clathrin-mediated endocytosis as the main route for agonist-promoted removal of cell surface CB_1Rs. More recent studies demonstrated that agonist-promoted CB_1R internalization can occur via both clathrin and caveolin pathways, which together were reported to account for endocytosis of ~ 40% of receptors (Keren and Sarne 2003; Wu *et al.* 2008). Our assays are based on an antibody interaction with the CB_1R N-terminus, which would not be accessible after a coated pit has closed in a dynamin-dependent mechanism. In addition to CRIP1a's function to suppress agonist-mediated internalization of CB_1Rs, a recent disclosure indicated that the Src homology 3-domain growth factor receptor-bound 2-like (endophilin)-interacting protein 1 can also interact with the CB_1R to inhibit agonist-driven, clathrin-mediated endocytosis of the CB_1R (Hajkova *et al.* 2016).

We previously reported that exogenous CRIP1a over-expression could attenuate CB_1R down-regulation but not desensitization (Smith *et al.* 2015). Prolonged treatment with cannabinoid agonists leads to CB_1R down-regulation in rodent brains, as evidenced by decreases in CB1R immunoblotting and [^{3}H]rimonabant B_{max} values (Sim-Selley *et al.* 2006). Delta9-Tetrahydrocannabinol-induced down-regulation of CB_1Rs was attenuated in the cerebellum and spinal cord of β-arrestin2 knockout mice relative to WT littermates (Nguyen *et al.* 2012). Martini *et al.* (2007) reported evidence that binding of GASP1 to the CB_1R resulted in CB_1R trafficking to lysosomes and receptor degradation during prolonged treatment with WIN55212-2. Our finding that the re-establishment of cell surface CB_1R levels during extended periods of agonist exposure requires *de novo* synthesis is consistent with the degradation, rather than recycling, of internalized receptors, and is consistent with the degradation of internalized receptors reported from studies of AtT20 cells and the striatum of ICR mice (Hsieh *et al.* 1999; Sim-Selley *et al.* 2006).

In agreement with previous work performed in HEK293 and primary cultured neurons (Martini *et al.* 2007), we discovered that there were agonist-specific differences in the return of cell surface CB_1Rs to steady-state levels: CB_1R surface expression returned to pre-agonist levels following prolonged treatment with CP55940, but not WIN55212-2. The failure of WIN55212-2-occupied CB_1R to re-establish pre-agonist steady-state plasma membrane levels could be overcome if CRIP1a expression was reduced below endogenous levels (Fig. 5d). This suggests that CRIP1a at endogenous levels serves a function to suppress plasma

membrane CB_1R. One mechanism is that CRIP1a could increase the rate of degradation of plasma membrane CB_1Rs. This possibility is unlikely, because: (i) CRIP1a over-expression suppresses internalization (Fig. 1) which is required as a first step leading to degradation; and (ii) CRIP1a over-expression in the HEK293 cell model reduced CB_1R down-regulation (Smith *et al.* 2015). Martini *et al.* (2007) determined that agonist-promoted down-regulation of CB_1R over a similar time course in HEK293 cells was mediated by the association of CB_1R with GASP1, resulting in targeting the receptor to the lysosomal degradation pathway.

A more likely mechanism for the suppression of cell surface CB_1R levels by CRIP1a over-expression, as well as the ability of CRIP1a knockdown to rescue CB_1R steady-state levels following prolonged WIN55212-2 treatment, is that CRIP1a could suppress the trafficking of nascent CB_1R to the plasma membrane. Early studies identified a pool of CB_1Rs in N18TG2 neuronal cells that are localized in the perinuclear compartment (McIntosh *et al.* 1998), potentially providing a source of receptors that could be translocated to the plasma membrane. The re-appearance of CB_1Rs on the cell surface after prolonged agonist exposure may be because of translocation of newly synthesized receptors sequestered this pool.

The ability of rimonabant to increase CB_1R cell surface expression has been attributed to its inverse agonist effects to block 'constitutive' internalization of CB_1Rs (Rinaldi-Carmona *et al.* 1998; Leterrier *et al.* 2004; McDonald *et al.* 2007). We did not observe any significant influence of CRIP1a levels on the rate or extent of the transient increase in CB_1R density at the cell surface by rimonabant (Fig. 7). The experiments reported herein were conducted by removal of serum to eliminate variability in exposure to that source of endocannabinoids, as well as THL to inhibit diacylglycerol lipase and reduce 2-arachidonoylglycerol (2-AG) levels (Smith *et al.* 2015). These precautions reduce 'endocannabinoid tone' that could activate the CB_1R. Gyombolai *et al.* (2013) found that clathrin was required for both exogenous agonist- and non-agonist-stimulated internalization of CB_1R in Neuro2A and HeLa cells, whereas β-arrestin2 was required only for agonist-driven but not the 'constitutive' internalization of CB_1R. Thus, there may be differences between the agonist-stimulated versus non-agonist-mediated internalization that allows CRIP1a to regulate agonist-driven events alone. The data showing that rimonabant could overcome CRIP1a-mediated suppression of CB_1R cell surface steady state (Fig. 7a) suggest that binding of rimonabant to the CB_1R can preclude or reverse the influence of CRIP1a. Although there may be complex interpretations of 'constitutive' activity versus 'constitutive' internalization in the absence of exogenous agonists, or 'endocannabinoid tone' resulting in autocrine or paracrine responses, our studies of transgenic cells altered in CRIP1a expression demonstrate a CRIP1a regulation of steady-state cell surface CB_1R in the N18TG2 neuronal model. Our findings provide a rationale to investigate the influence of CRIP1a on CB_1R in more complex *in vivo* animal models.

Overall, these findings identify a novel function for CRIP1a in regulating agonist-promoted CB_1R internalization. We propose that CRIP1a serves to fine-tune the extent of CB_1R internalization and cell surface expression. Our data suggest that CRIP1a also functions in the delivery of newly synthesized CB_1Rs. Drug development using CB_1R agonists and antagonists has had limited success because of untoward side effects. The ability of CRIP1a to modulate CB_1R cell surface levels in those cell types that express CRIP1a suggests that

changes in CRIP1a expression could provide a mechanism to modulate CB_1R abundance on the cell surface, and offers a potentially promising approach to the development of more selective CB_1R pharmacotherapies. Future studies will determine whether CRIP1a has any interactions with GASP1 or Src homology 3-domain growth factor receptor-bound 2-like (endophilin)-interacting protein 1, or how CRIP1a may be involved with the AP-2 complex and associated adaptor proteins such as β-arrestin, ARF and Rho G proteins, epsin, amphiphysins and Eps15 (Kelly and Owen 2011; Croise *et al.* 2014; Paczkowski *et al.* 2015). Further investigation is necessary to address issues of differences in CB_1R expression levels particularly between endogenously expressed versus stably transfected receptors in host cell models, biased ligand influences, treatment time courses and other cell regulatory influences.

Acknowledgments

We are grateful for access to the Microscopic Imaging Core Facility of the Wake Forest University Biology Department. This work was supported by the US Public Health Service grants R01-DA03690, R21-DA025321, R03-DA035424, K01-DA024763, T32-DA007246, T32-AA007565, F31-DA032215, and funding from the Wake Forest University Center for Molecular Signaling.

References

Bari M, Battista N, Fezza F, Finazzi-Agro A, Maccarrone M. Lipid rafts control signaling of type-1 cannabinoid receptors in neuronal cells. Implications for anandamide-induced apoptosis. J Biol Chem. 2005; 280:12212–12220. [PubMed: 15657045]

Blume LC, Bass CE, Childers SR, Dalton GD, Roberts DC, Richardson JM, Xiao R, Selley DE, Howlett AC. Striatal CB1 and D2 receptors regulate expression of each other, CRIP1A and delta opioid systems. J Neurochem. 2013; 124:808–820. [PubMed: 23286559]

Blume LC, Eldeeb K, Bass CE, Selley DE, Howlett AC. Cannabinoid receptor interacting protein (CRIP1a) attenuates CB1R signaling in neuronal cells. Cell Signal. 2015; 27:716–726. [PubMed: 25446256]

Coutts AA, Anavi-Goffer S, Ross RA, MacEwan DJ, Mackie K, Pertwee RG, Irving AJ. Agonist-induced internalization and trafficking of cannabinoid CB1 receptors in hippocampal neurons. J Neurosci. 2001; 21:2425–2433. [PubMed: 11264316]

Croise P, Estay-Ahumada C, Gasman S, Ory S. Rho GTPases, phosphoinositides, and actin: a tripartite framework for efficient vesicular trafficking. Small GTPases. 2014; 5:e29469. [PubMed: 24914539]

Cuitino L, Matute R, Retamal C, Bu G, Inestrosa NC, Marzolo MP. ApoER2 is endocytosed by a clathrin-mediated process involving the adaptor protein Dab2 independent of its Rafts' association. Traffic. 2005; 6:820–838. [PubMed: 16101684]

Daigle TL, Kwok ML, Mackie K. Regulation of CB1 cannabinoid receptor internalization by a promiscuous phosphorylation-dependent mechanism. J Neurochem. 2008; 106:70–82. [PubMed: 18331587]

Delgado-Peraza F, Ahn KH, Nogueras-Ortiz C, Mungrue IN, Mackie K, Kendall DA, Yudowski GA. Mechanisms of biased beta-arrestin-mediated signaling downstream from the cannabinoid 1 receptor. Mol Pharmacol. 2016; 89:618–629. [PubMed: 27009233]

Drake MT, Shenoy SK, Lefkowitz RJ. Trafficking of G protein-coupled receptors. Circ Res. 2006; 99:570–582. [PubMed: 16973913]

Flores-Otero J, Ahn KH, Delgado-Peraza F, Mackie K, Kendall DA, Yudowski GA. Ligand-specific endocytic dwell times control functional selectivity of the cannabinoid receptor 1. Nat Commun. 2014; 5:4589. [PubMed: 25081814]

Gold ES, Underhill DM, Morrissette NS, Guo J, McNiven MA, Aderem A. Dynamin 2 is required for phagocytosis in macrophages. J Exp Med. 1999; 190:1849–1856. [PubMed: 10601359]

Gyombolai P, Boros E, Hunyady L, Turu G. Differential beta-arrestin2 requirements for constitutive and agonist-induced internalization of the CB1 cannabinoid receptor. Mol Cell Endocrinol. 2013; 372:116–127. [PubMed: 23541635]

Hajkova A, Techlovska S, Dvorakova M, Chambers JN, Kumpost J, Hubalkova P, Prezeau L, Blahos J. SGIP1 alters internalization and modulates signaling of activated cannabinoid receptor 1 in a biased manner. Neuropharmacology. 2016; 107:201–214. [PubMed: 26970018]

Hanyaloglu AC, von Zastrow M. Regulation of GPCRs by endocytic membrane trafficking and its potential implications. Annu Rev Pharmacol Toxicol. 2008; 48:537–568. [PubMed: 18184106]

Howlett AC, Blume LC, Dalton GD. CB1 cannabinoid receptors and their associated proteins. Curr Med Chem. 2010; 17:1382–1393. [PubMed: 20166926]

Hsieh C, Brown S, Derleth C, Mackie K. Internalization and recycling of the CB1 cannabinoid receptor. J Neurochem. 1999; 73:493–501. [PubMed: 10428044]

Jin W, Brown S, Roche JP, Hsieh C, Celver JP, Kovoor A, Chavkin C, Mackie K. Distinct domains of the CB1 cannabinoid receptor mediate desensitization and internalization. J Neurosci. 1999; 19:3773–3780. [PubMed: 10234009]

Kelly BT, Owen DJ. Endocytic sorting of transmembrane protein cargo. Curr Opin Cell Biol. 2011; 23:404–412. [PubMed: 21450449]

Keren O, Sarne Y. Multiple mechanisms of CB1 cannabinoid receptors regulation. Brain Res. 2003; 980:197–205. [PubMed: 12867259]

Leterrier C, Bonnard D, Carrel D, Rossier J, Lenkei Z. Constitutive endocytic cycle of the CB1 cannabinoid receptor. J Biol Chem. 2004; 279:36013–36021. [PubMed: 15210689]

Leterrier C, Laine J, Darmon M, Boudin H, Rossier J, Lenkei Z. Constitutive activation drives compartment-selective endocytosis and axonal targeting of type 1 cannabinoid receptors. J Neurosci. 2006; 26:3141–3153. [PubMed: 16554465]

Martini L, Waldhoer M, Pusch M, Kharazia V, Fong J, Lee JH, Freissmuth C, Whistler JL. Ligand-induced down-regulation of the cannabinoid 1 receptor is mediated by the G-protein-coupled receptor-associated sorting protein GASP1. FASEB J. 2007; 21:802–811. [PubMed: 17197383]

Mayor S, Pagano RE. Pathways of clathrin-independent endocytosis. Nat Rev Mol Cell Biol. 2007; 8:603–612. [PubMed: 17609668]

McDonald NA, Henstridge CM, Connolly CN, Irving AJ. An essential role for constitutive endocytosis, but not activity, in the axonal targeting of the CB1 cannabinoid receptor. Mol Pharmacol. 2007; 71:976–984. [PubMed: 17182888]

McIntosh HH, Song C, Howlett AC. CB1 cannabinoid receptor: cellular regulation and distribution in N18TG2 neuroblastoma cells. Brain Res Mol Brain Res. 1998; 53:163–173. [PubMed: 9473654]

Miller JW. Tracking G protein-coupled receptor trafficking using Odyssey (R) imaging. 2004

Nguyen PT, Schmid CL, Raehal KM, Selley DE, Bohn LM, Sim-Selley LJ. beta-arrestin2 regulates cannabinoid CB1 receptor signaling and adaptation in a central nervous system region-dependent manner. Biol Psychiatry. 2012; 71:714–724. [PubMed: 22264443]

Niehaus JL, Liu Y, Wallis KT, et al. CB1 cannabinoid receptor activity is modulated by the cannabinoid receptor interacting protein CRIP 1a. Mol Pharmacol. 2007; 72:1557–1566. [PubMed: 17895407]

Paczkowski JE, Richardson BC, Fromme JC. Cargo adaptors: structures illuminate mechanisms regulating vesicle biogenesis. Trends Cell Biol. 2015; 25:408–416. [PubMed: 25795254]

Rejman J, Bragonzi A, Conese M. Role of clathrin- and caveolae-mediated endocytosis in gene transfer mediated by lipo-and polyplexes. Mol Ther. 2005; 12:468–474. [PubMed: 15963763]

Rinaldi-Carmona M, Le Duigou A, Oustric D, Barth F, Bouaboula M, Carayon P, Casellas P, Le Fur G. Modulation of CB1 cannabinoid receptor functions after a long-term exposure to agonist or inverse agonist in the Chinese hamster ovary cell expression system. J Pharmacol Exp Ther. 1998; 287:1038–1047. [PubMed: 9864290]

Sarnataro D, Grimaldi C, Pisanti S, Gazzerro P, Laezza C, Zurzolo C, Bifulco M. Plasma membrane and lysosomal localization of CB1 cannabinoid receptor are dependent on lipid rafts and regulated by anandamide in human breast cancer cells. FEBS Lett. 2005; 579:6343–6349. [PubMed: 16263116]

Sim-Selley LJ, Schechter NS, Rorrer WK, Dalton GD, Hernandez J, Martin BR, Selley DE. Prolonged recovery rate of CB1 receptor adaptation after cessation of long-term cannabinoid administration. Mol Pharmacol. 2006; 70:986–996. [PubMed: 16760363]

Smith TH, Sim-Selley LJ, Selley DE. Cannabinoid CB1 receptor-interacting proteins: novel targets for central nervous system drug discovery? Br J Pharmacol. 2010; 160:454–466. [PubMed: 20590557]

Smith TH, Blume LC, Straiker A, et al. Cannabinoid receptor-interacting protein 1a modulates CB1 receptor signaling and regulation. Mol Pharmacol. 2015; 87:747–765. [PubMed: 25657338]

Stadel R, Ahn KH, Kendall DA. The cannabinoid type-1 receptor carboxyl-terminus, more than just a tail. J Neurochem. 2011; 117:1–18. [PubMed: 21244428]

Wang LH, Rothberg KG, Anderson RG. Mis-assembly of clathrin lattices on endosomes reveals a regulatory switch for coated pit formation. J Cell Biol. 1993; 123:1107–1117. [PubMed: 8245121]

Wu DF, Yang LQ, Goschke A, Stumm R, Brandenburg LO, Liang YJ, Hollt V, Koch T. Role of receptor internalization in the agonist-induced desensitization of cannabinoid type 1 receptors. J Neurochem. 2008; 104:1132–1143. [PubMed: 17986216]

Abbreviations

AP-3	adaptor protein 3
CB_1R	CB_1 cannabinoid receptor
CP55940	(-)-*cis*-3-[2-hydroxy-4-(1,1-dimethylheptyl)phenyl]-*trans*-4-(3-hydroxypropyl)cyclohexanol
CPZ	chlorpromazine
CRIP1a	cannabinoid receptor interacting protein 1a
dynasore	3-hydroxy-naphthalene-2-carboxylic acid (3,4-dihydroxybenzylidene) hydrazide
GASP1	GPCR-associated sorting protein 1
GPCR	G-protein-coupled receptor
GRK	GPCR kinase
rimonabant	N-(piperidin-1-yl)-5-(4-chlorophenyl)-1-(2,4-dichlorophenyl)-4-methyl-1H-pyrazole-3-carboxamide
RNAi	RNA interference
THL	tetrahydrolipstatin
WIN55212-2	[2,3-dihydro-5-methyl-3-[(4-morpholinyl)methyl]pyrrolo[1,2,3-de]-1,4-benzoxazin-6-yl](1-naphthyl) methanone
WT	untransfected wild-type cells

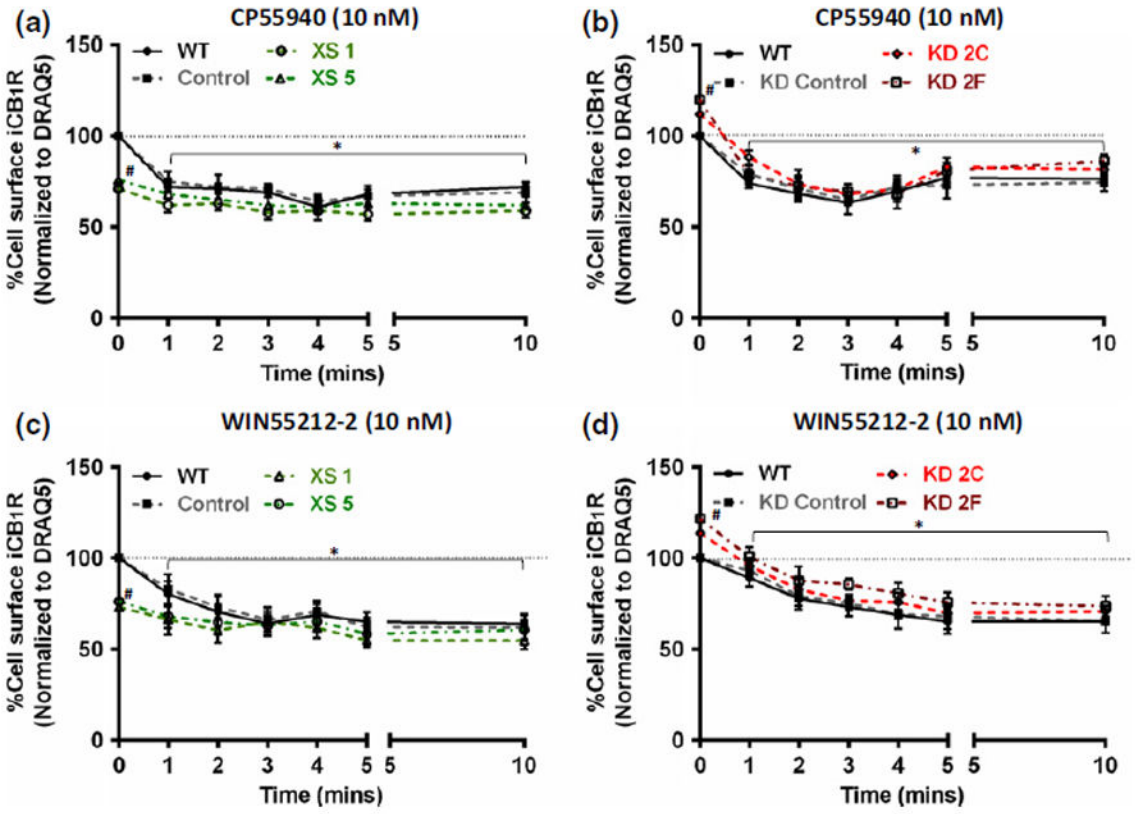

Fig. 1.

CRIP1a affects agonist-promoted loss of cell surface CB_1R. N18TG2 wild-type (WT, untransfected), empty vector control, CRIP1a XS (a and c) and CRIP1a KD (b and d) clones were treated with CP55940 (10 nM) (a and b) or WIN 55212-2 (10 nM) (c and d) at time 0. Cell surface CB_1R was quantitated at indicated times as the ratio of extracellular immunoreactive CB_1R to DRAQ5. Time courses for individual transgenic clones were calculated independently by normalizing to time 0, and expressed as 100% for WT at time 0. Data are presented as the mean ± SEM from three independent experiments performed in triplicate. *$p < 0.05$, data points within the solid line above WT and control (a, c), and WT, control and CRIP1a KD cells (b, d) significantly differ from time 0 for each clone. No significant differences from time 0 were observed at any time point for CRIP1a XS clones. #$p < 0.05$, indicates significant difference between CRIP1a XS and WT (a, c) or CRIP1a KD and WT (b, d) at time = 0, using Student's *t*-test.

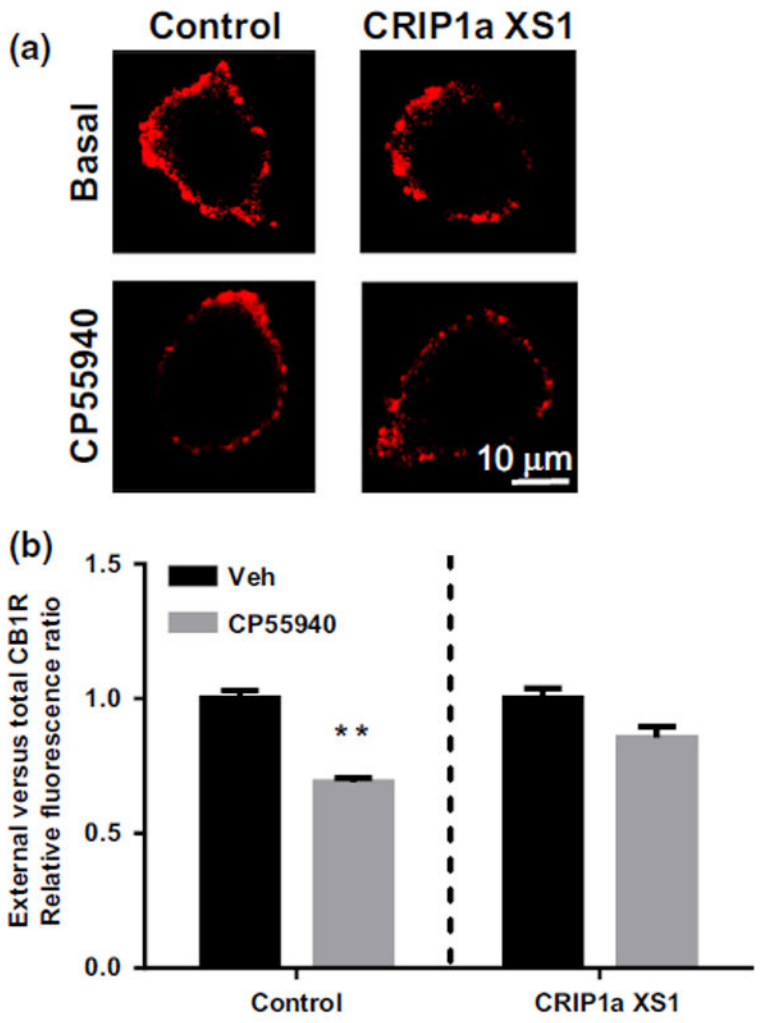

Fig. 2.

CRIP1a over-expression attenuates agonist-promoted CB_1R cell surface depletion. N18TG2 empty vector control, and CRIP1a XS cells were treated with vehicle (Veh) or CP55940 (10 nM) for 15 min (a). Surface CB_1Rs were fluorescently labeled (red) as described in Materials and methods. The scale bar for images is 10 µm. (b) Control or CRIP1a XS cells were treated with vehicle or CP55940 (10 nM) for 5 min, and external CB_1Rs were labeled with a goat N-terminal CB_1R antibody, followed by fixation, permeabilization and labeling of total CB_1Rs with a rabbit C-terminal CB_1R antibody. Quantification is reported as the mean ratio of external/total fluorescence of cells examined across four fields from 1 or 2 coverslips each in three independent experiments, for a total of 48–60 cells per condition. $^{**}p < 0.01$ significantly different CP55940 versus vehicle ANOVA with Bonferroni *post hoc* test.

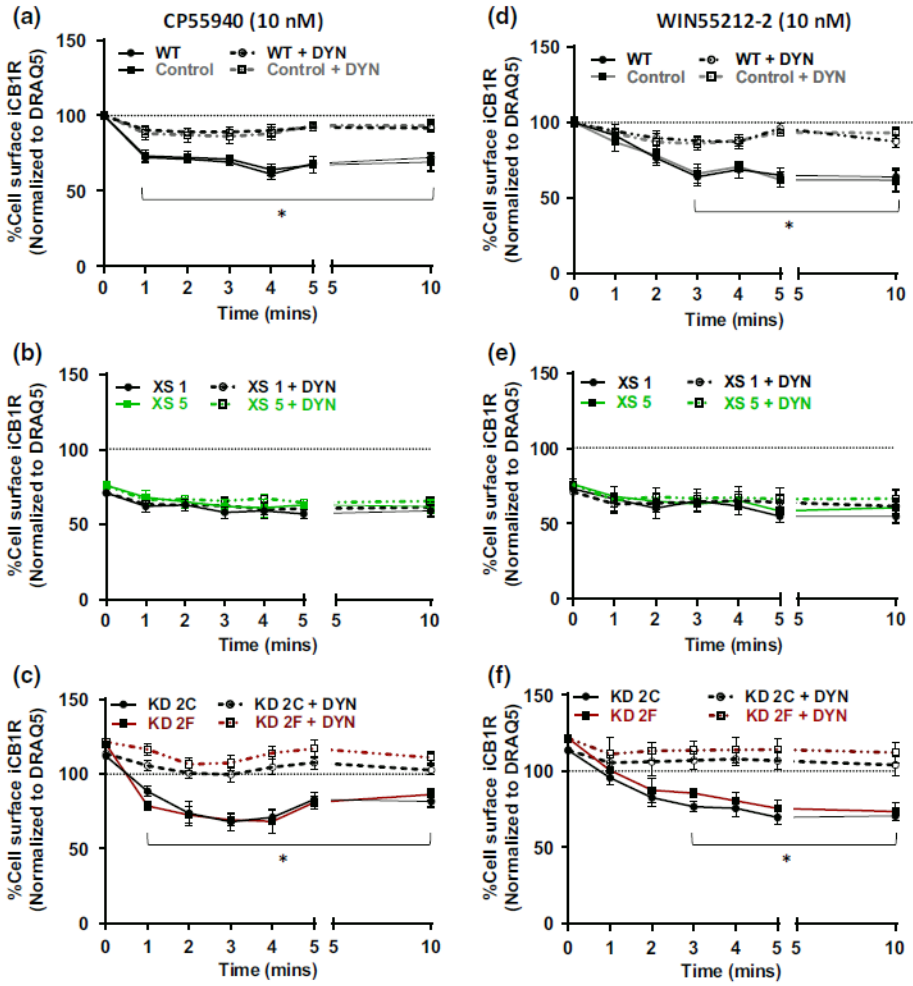

Fig. 3.

CRIP1a modulates agonist-promoted, dynamin-dependent CB_1R cell surface depletion. N18TG2 wild-type (WT) and empty vector control cells (a, d), CRIP1a XS (b, e) and CRIP1a KD clones (c, f) were pretreated for 30 min with vehicle or the dynamin inhibitor dynasore (80 μM), and challenged with the CB_1R agonists CP55940 (10 nM) (a–c) or WIN55212-2 (10 nM) (d–f) for the indicated times. CB_1R cell surface density was quantitated using the On-cell-Western assay, and CB_1R surface expression was determined as the ratio of immunoreactive CB_1R to DRAQ5, represented as 100% at time 0 for WT. Time course data were compared independently to time 0 for each transgenic clone. In (a, c, d, f) $*p < 0.05$, the solid line below untreated WT, control and CRIP1a KD cells indicates that inclusive data points significantly differ from time 0 for WT, Control and CRIP1aKD cells using Student's *t*-test. (b and e) No significant differences from time 0 were detected in CRIP1aXS clones in the presence or absence of dynasore. (a–f) No significant differences from time 0 were detected for dynasore-treated cells for any of the clones. Data are presented as the mean ± SEM from four independent experiments performed in duplicate.

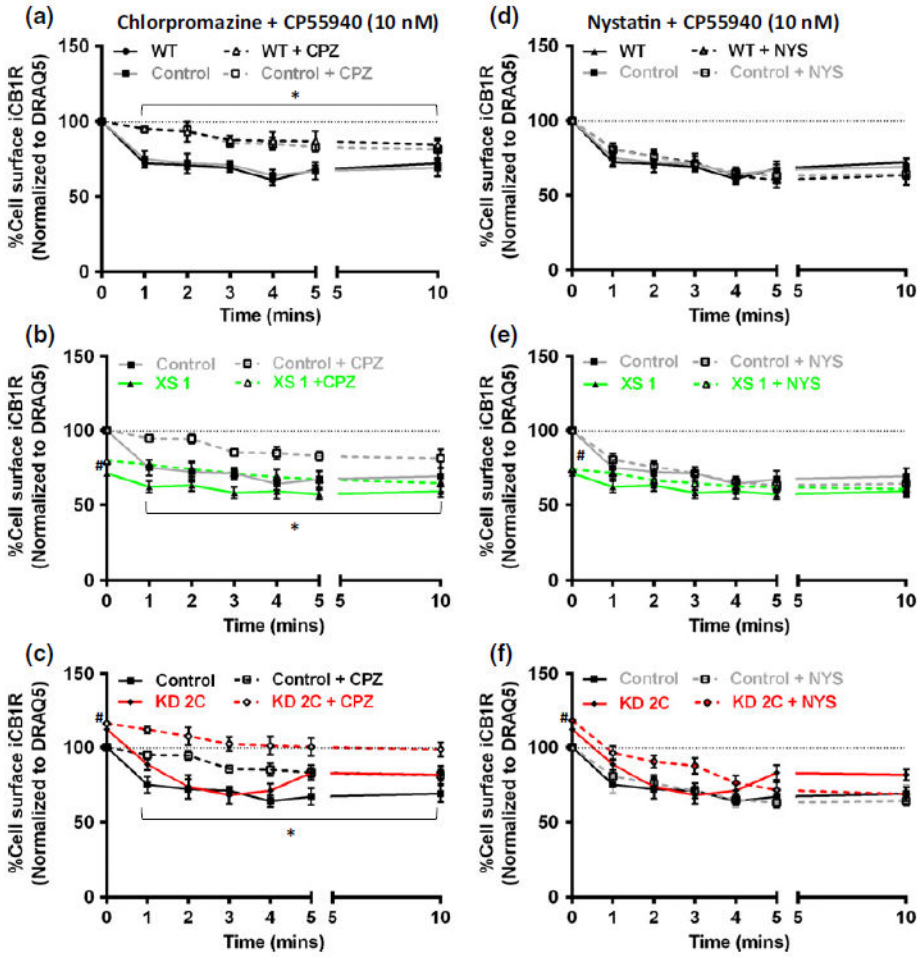

Fig. 4.

CRIP1a modulates agonist-promoted CB_1R loss through a clathrin-mediated but not caveolin-mediated mechanism. Cells were pretreated for 30 min with vehicle (DMSO), 25 μM chlorpromazine (CPZ, a–c) or 25 μM nystatin (NYS, d–f), and challenged for the indicated times with CP55940 (10 nM). On-cell-Western analysis of CB_1R cell surface expression was quantitated as described in Materials and methods. Time courses for individual transgenic clones were calculated independently by normalizing to time 0, and expressed as 100% for wild type (WT) at time 0. Data are presented as the mean ± SEM calculated from three independent experiments performed in triplicate. #Indicates a significant difference $p < 0.05$ at time point 0 between CRIP1a XS and WT (b, e) and between WT and CRIP1a KD (c, f) clones. *Indicates time points within the solid line for WT and control (a), control (b) and control or CRIP1a KD (c) at which CPZ-treated were significantly different from non-treated values ($p < 0.05$) using Student's *t*-test. No significant differences were observed between CPZ-treated and non-treated values in CRIP1a XS cells (b). No significant differences were observed between NYS-treated and non-treated values in any cell clones (d–f).

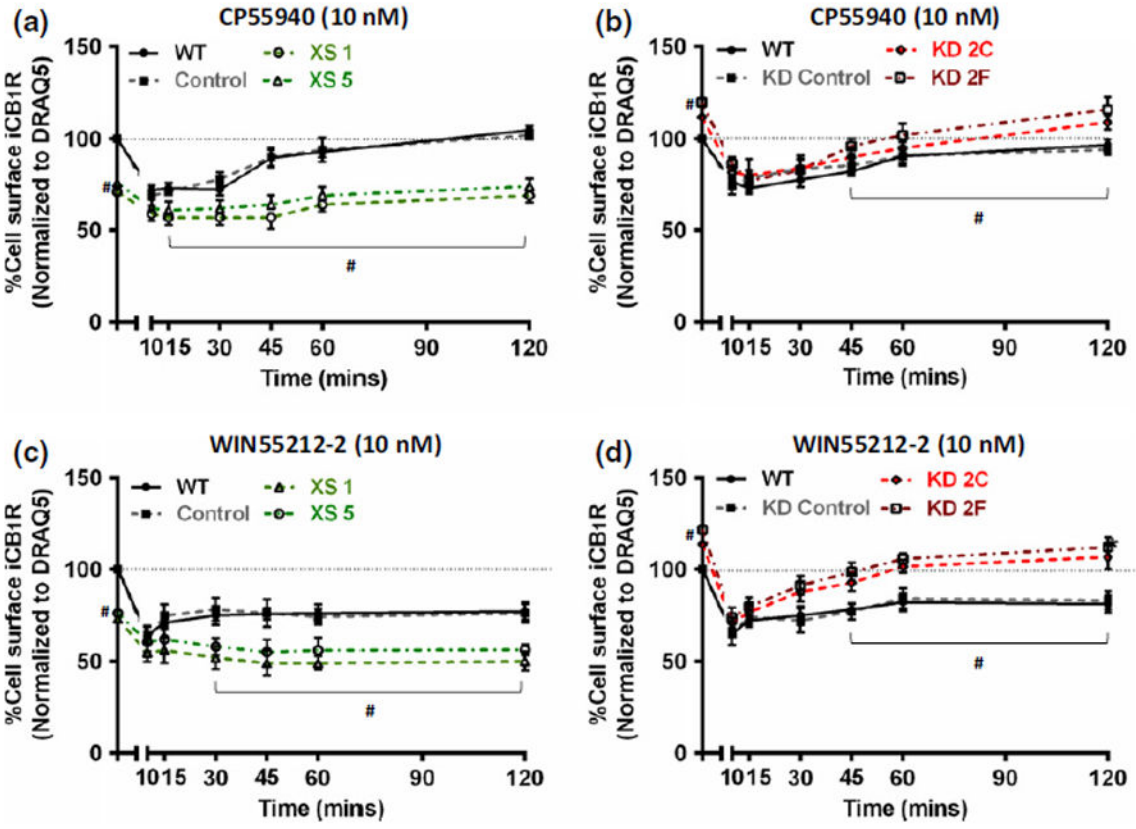

Fig. 5.

CRIP1a modulates CB_1R surface recovery during agonist challenge in an agonist-dependent manner. An extended time course is shown for CP55940- (a and b) or WIN55212-2 (c and d) mediated CB_1R cell surface levels in N18TG2 wild-type (WT), empty vector control, CRIP1a XS (a and c) and CRIP1a KD (b and d) clones. Cells were serum-starved for 16 h, pretreated with 1 μM tetrahydrolipstatin for 2 h, and treated with 10 nM of the CB_1R agonist CP55940 or WIN55212-2 for the indicated times. CB_1R cell surface expression was quantitated using the On-cell-Western assay, and determined as the ratio of immune-reactive CB_1R to DRAQ5 fluorescence. Time courses for individual transgenic clones were calculated independently by normalizing to time 0, and expressed as 100% for WT at time 0. Data are presented as the mean ± SEM from three independent experiments performed in triplicate. #$p < 0.05$, the solid line indicates significant difference between CRIP1a XS and WT (a, c) or CRIP1a KD and WT (b, d) at the same time point, using Student's *t*-test.

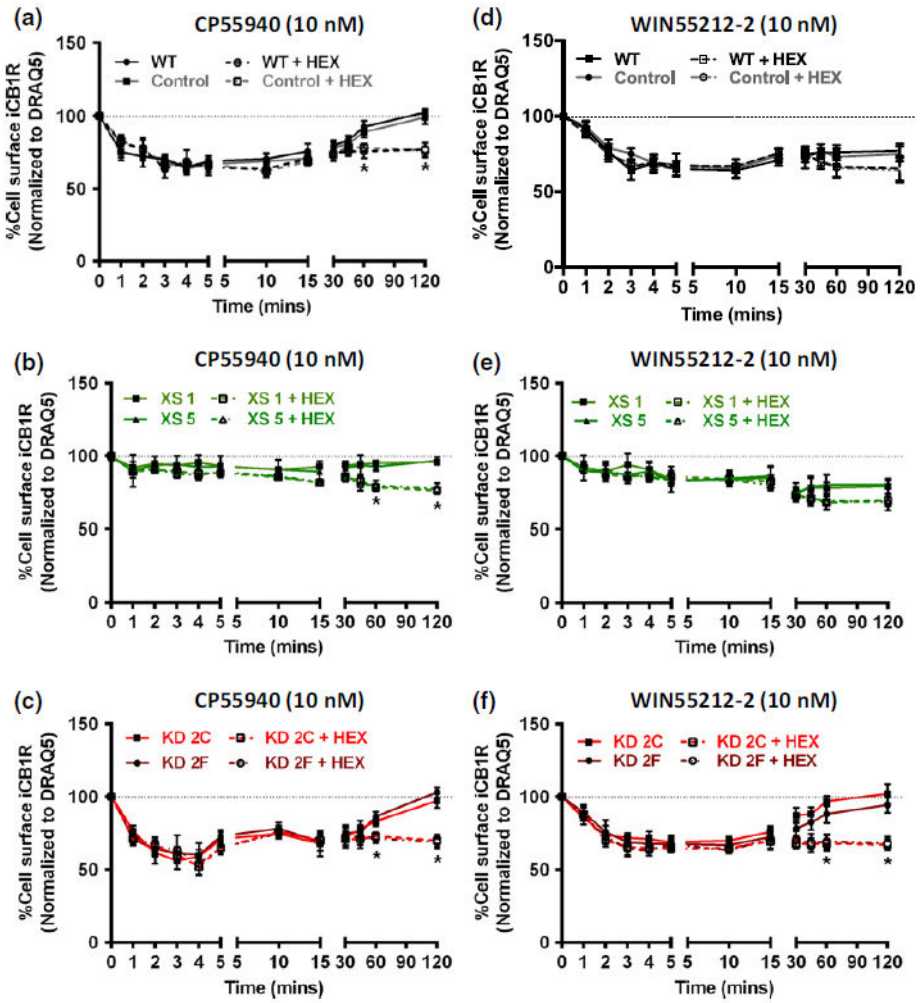

Fig. 6.

De novo CB_1R synthesis is required for re-establishing surface membrane receptor density during prolonged agonist exposure. N18TG2 wild-type (WT), empty vector control (a and d), CRIP1a XS (b and e) and CRIP1a KD (c and f) clones were pretreated for 30 min with vehicle or the protein synthesis inhibitor cycloheximide (HEX) (1 μM), and then challenged for the indicated times with the CP55940 (10 nM) (a–c) or WIN55212-2 (10 nM) (d–f). CB_1R cell surface levels were quantitated by On-cell Western assays, and determined as % of CB_1R at time 0, and expressed as 100% for each clone individually at time 0. Data are calculated from three independent experiments performed in triplicate, and represented as the mean ± SEM. $*p < 0.05$ indicates time points at which HEX values were significantly different from non-treated using Student's *t*-test.

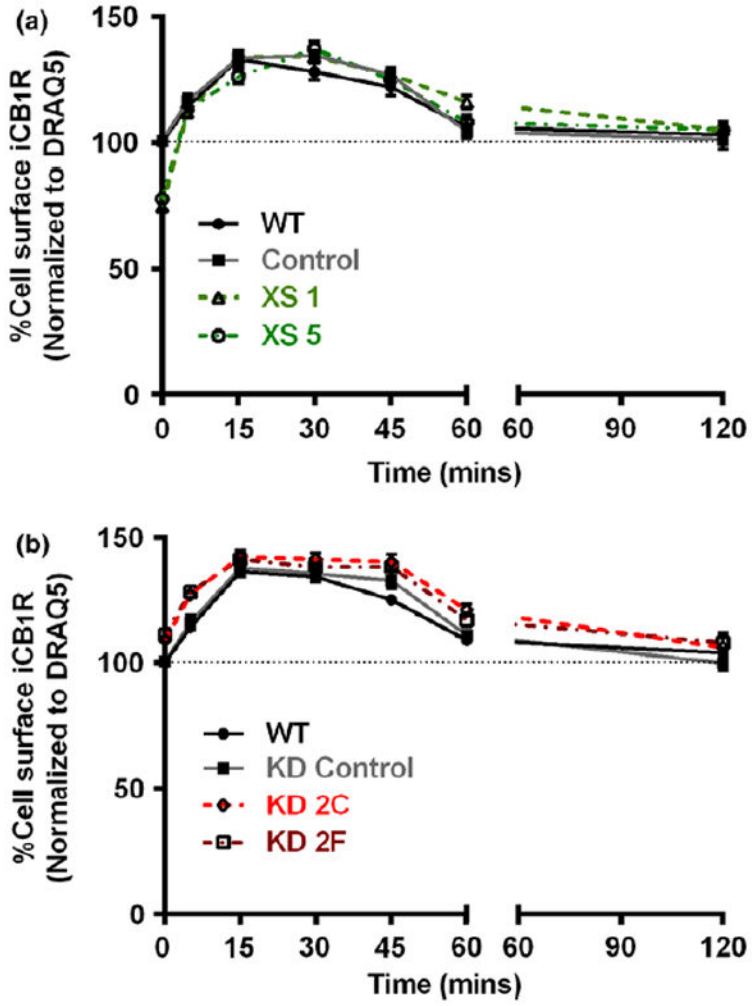

Fig. 7.

CRIP1a levels do not influence inverse agonist-promoted increase in cell surface CB_1R density. The time course for rimonabant-mediated changes in CB_1R cell surface expression compares N18TG2 wild-type (WT) and empty vector Control to CRIP1 XS clones (a), and CRIP1a KD clones (b). Cells were pretreated with 1 μM tetrahydrolipstatin for 2 h, and then challenged with the CB_1R antagonist rimonabant (10 nM) for the indicated times. Quantification of CB_1R cell surface expression was determined using the On-cell-Western assay. Each time point was normalized to time 0 for each clone, but expressed as 100% for WT at time 0. The mean ± SEM were calculated from four independent experiments performed in triplicate. No significant differences were observed between WT, CRIP1a XS, and CRIP1a KD clones at any time point, except time 0 ($p < 0.05$, Student's *t*-test).